Multidimensional Crystal Engineering of Bifunctional Metal Complexes Containing Complementary Triple Hydrogen Bonds

Andrew D. Burrows, Chin-Wing Chan, Mubarik M. Chowdhry, John E. McGrady, and D. Michael P. Mingos*

Department of Chemistry, Imperial College of Science, Technology and Medicine, South Kensington, London SW7 2AY, U.K.

1 Introduction

The control of molecular assembly using supramolecular interactions is a major new area in chemistry and biochemistry.[1] In particular, the directional interactions resulting from hydrogen bonding are being exploited for molecular recognition studies associated with biological activity[2] and for crystal engineering of solids.[3] The design of organic molecular solids utilising the self-assembly of molecules which contain complementary hydrogen bonding groups structurally related to those found in nucleic acid base pairs is a common feature in the research work of Whitesides,[4] Lehn,[5] Hamilton,[6] and their co-workers. Excellent reviews describing the application of biologically inspired hydrogen bonding models for developing molecular recognition strategies are to be found in references 7—10. This review describes the extension of this principle to transition metal containing complexes. The incorporation of transition metal ions into such systems is important because the magnetic and optical properties characteristic of these ions become part of a broader strategy for the crystal engineering of nonlinear optical, conducting, and ferromagnetic materials. In addition the biological effects associated with, for example, platinum and gold, could lead to some interesting new chemotherapeutic possibilities.

Specifically we have a synthetic, structural, and theoretical programme of research aimed at synthesizing bifunctional transition metal complexes, which combine the covalent bond forming capabilities of the metal ion with a ligand surface capable of forming triple hydrogen bonds analogous to those found in cytosine–guanine base pairs (1) and related permutations.

Target complexes which satisfy these structural requirements are illustrated in (2)—(7) in Figure 1. In (2) the complex has a donor (D)–acceptor (A)–donor (D) hydrogen bonding capabi-

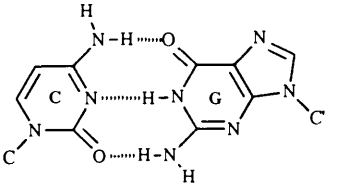

(1)

Andrew Burrows was born in Ipswich, Suffolk in 1966. He obtained his B.A. (1988) and D. Phil. (1992) from the University of Oxford, the latter on the chemistry of palladium cluster compounds under the supervision of Professor Mingos. He then worked as a Royal Society/Elf Aquitaine European Exchange Fellow at the Université Louis Pasteur, Strasbourg with Dr. P. Braunstein and currently holds a Fixed Term Lectureship at Imperial College where his current research interests are supramolecular coordination chemistry and cluster chemistry.

Chin-Wing Chan was born in Hong Kong. He obtained his B.Sc. (Hons. 1985) and M. Phil. (1987) from the Chinese University of Hong Kong where he was trained in organic synthesis by Professor Henry N. C. Wong. After working for three years at Hong Kong Baptist College, he joined Professor Chi-Ming Che's research team in the University of Hong Kong to study photophysical and photochemical properties of cyclometallated d^8 transition metal complexes (Ph.D. 1994). Now he is completing the Croucher Fellowship with Professor Mingos at Imperial College. His research focus covers coordination chemistry with designed ligands that can participate in molecular self-assembly.

John McGrady was born in Newcastle upon Tyne in 1968. He obtained his BA from the University of Oxford in 1990, and his Ph.D. from the Australian National University in 1994. He is currently a post-doctoral research associate at Imperial College, working on the applications of density functional theory to multiply hydrogen-bonded systems.

Mubarik Chowdhry was born in London in 1970. He obtained his B.Sc. from Imperial College in 1993. During his degree, he carried out research for The Dow Corning Corporation in Barry, Wales. In his final year, he carried out research for Professor J. A. Osborn in Strasbourg on Self-Assembly of Copper(I). He is currently a Post-graduate student under Professor Mingos at Imperial College, working on supramolecular coordination chemistry.

Michael Mingos is the Sir Edward Frankland B. P. Professor of Inorganic Chemistry at Imperial College of Science, Technology, and Medicine, London. He was appointed to this post in 1992 after 16 years as a lecturer and reader at the University of Oxford.

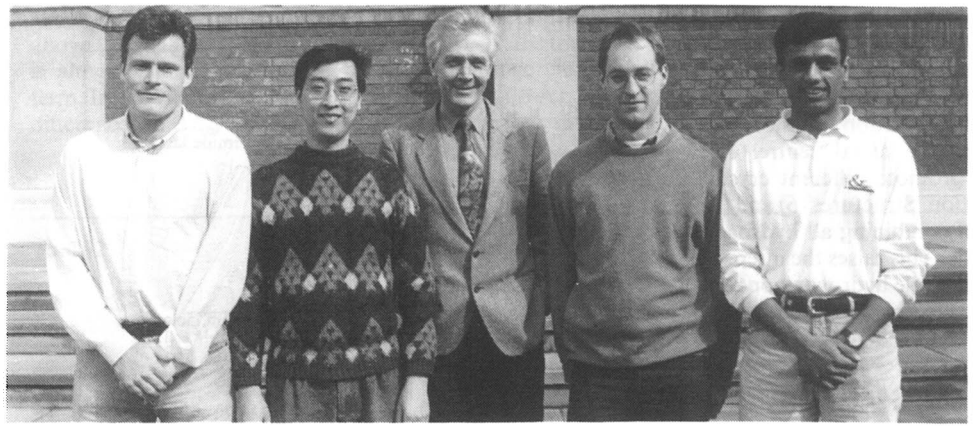

John McGrady **Chin-Wing Chan** **Michael Mingos** **Andrew Burrows** **Mubarik Chowdhry**

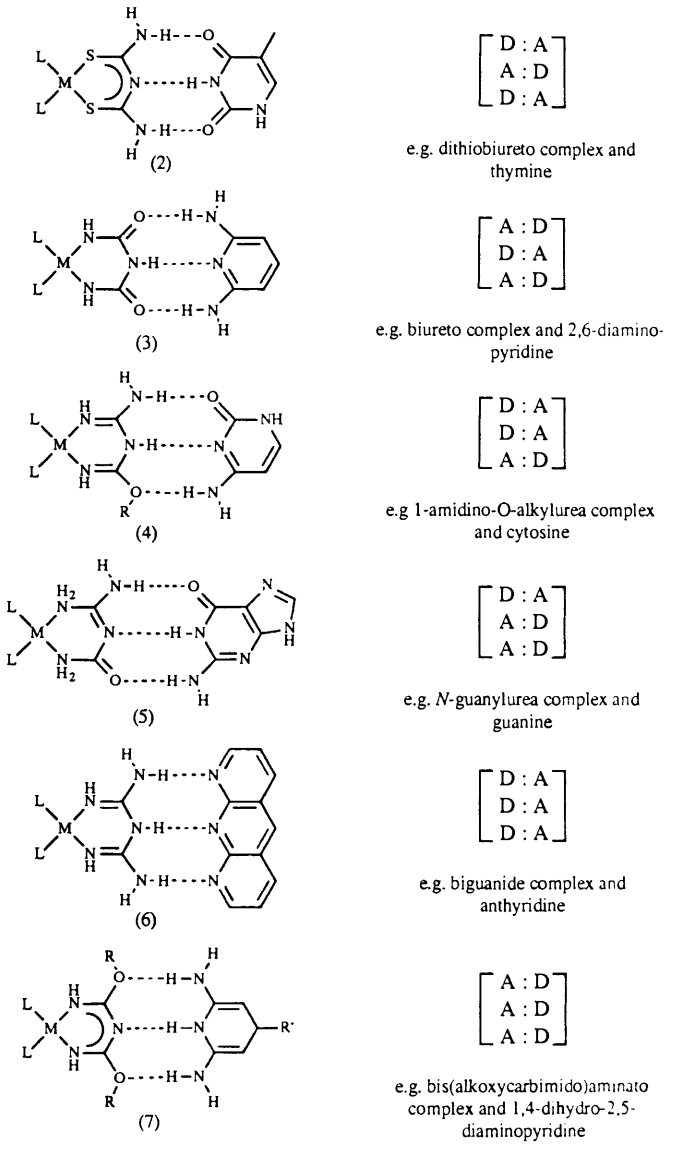

Figure 1 Triple hydrogen bonds between metal complexes and complementary organic molecules.

lity which complements that found in thymine for example, whereas (3) has an ADA hydrogen bonding recognition site which complements that in 2,6-diaminopyridine. Of course the metal complexes in (2) and (3) are themselves complementary. This raises the possibility of forming aggregates which combine the magnetic or electronic properties of quite different metal ions. Less symmetrical hydrogen bonding ligand recognition sites are also possible and are illustrated in (4) and (5). The complexes as shown in (2)—(5) have the molecular recognition group only on one face of the complex, but of course complexes which contain two or three ligands provide multiple recognition sites and oligomerization and polymerization possibilities. Alternative ligand geometries about the metal centre, *e.g.* square-planar and tetrahedral, will promote different crystal packing geometries after oligomerization. Structures (6) and (7) in Figure 1 indicate the possibility of combining all hydrogen donor or acceptor sites in one molecule. This raises the interesting question of how the strength of the triple hydrogen bonding interaction is affected by the different possible arrangements of donor and acceptor sites.

2 Theoretical Aspects

Accurate calculation of the noncovalent interactions prevalent in supramolecular systems provides a great challenge to conventional *ab initio* molecular orbital techniques. The need for an extended basis set, and also for an explicit treatment of electron correlation, means that extensive computational resources are required to treat the relatively large organic molecules relevant to the supramolecular field. Studies of DNA base pairs at the post-SCF level have recently been reported,[11] but such high quality calculations remain prohibitively expensive for a comparative study of a series of large complexes, particularly those incorporating transition metal ions. Molecular mechanics simulations offer a less expensive alternative for the estimation of interactions in supramolecular systems, and considerable effort has been made to develop suitable potential functions. In conjunction with the recently developed Statistical Perturbation Theory (SPT),[12] these empirical functions have provided quantitative estimates of free energies of association in solution. The widespread application of the SPT type calculations is, however, limited by the quality of the parameter set used to describe the potential function, and by the high cost of the computation.

Recent advances in Density Functional Theory[13] (DFT) have made possible the inclusion of electron correlation at substantially lower cost than traditional *ab initio* methods. Several groups have now shown that DFT can give accurate estimates of hydrogen bond energies and bond lengths.[14] In this section, we describe the application of DFT to a series of complexes relevant to the supramolecular field. The total bonding energy, ΔE_{tot}, between two fragments is decomposed according to the Transition State (TS) approach.[15]

$$\Delta E_{tot} = \Delta E_{el} + \Delta E_{xrp} + \Delta E_{oi} \quad (1)$$

ΔE_{el} represents the electrostatic interaction between the two monomeric fragments, while ΔE_{xrp}, the exchange repulsion term, results from the destabilizing interaction between occupied orbitals on different components. The final term, ΔE_{oi}, represents the interaction between occupied and virtual orbitals, and takes into account the transfer of electron density between fragments. The analysis of the components provides additional insight into the nature of the interactions, over and above that provided by simply calculating total interaction energies.

2.1 Double Hydrogen Bonded Systems

Association constants between imide and lactam molecular pairs (Figure 2) have been measured by several groups,[16] and complexes between two imides are consistently found to be less stable than their dilactam counterparts. SPT-type calculations

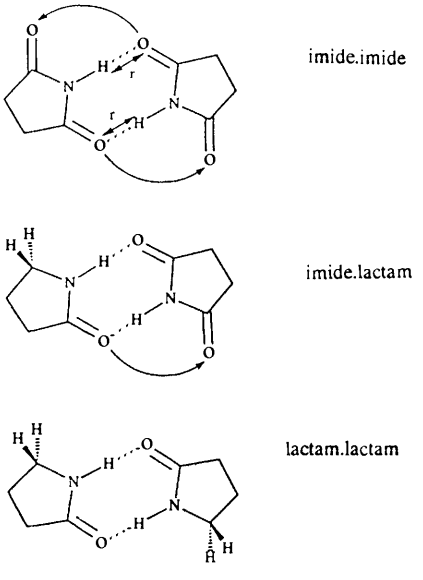

Figure 2 Hydrogen bonding between imide and lactam molecular pairs.

have successfully modelled the trend in association energies,[12a] and suggest that the differences are due to secondary electrostatic interactions between nonbonded oxygen atoms, indicated by the curved arrows in Figure 2. There are two such destabilizing interactions in imide.imide, one in imide.lactam, and none in the dilactam complex.

The decomposition of ΔE_{tot} at $r = 1.8$ Å is summarized in Table 1, and indicates that the DFT methodology successfully models the observed differences in interaction energy, with the diimide and dilactam complexes the least and most stable respectively. The components of the total energy indicate that the interaction is primarily electrostatic in nature, and that differences within this electrostatic term determine the overall trend in total bonding energy.[17] While these results do not eliminate the possibility that changes in the primary hydrogen bonds are responsible for the observed trends, the identification of the electrostatic component as the dominant influence lends support to the suggestion that secondary interactions involving nonbonded oxygens contribute significantly to variations in total energy. Variations in ΔE_{el} suggest a destabilizing effect of 10 kJmol^{-1} per secondary interaction, which compares favourably with the estimate of 11 kJmol^{-1} derived from the SPT methodology.

Table 1

	imide.imide	imide.lactam	lactam.lactam
ΔE_{el}	− 85.52	− 95.73	− 105.73
ΔE_{xrp}	108.53	112.26	115.44
ΔE_{oi}	− 71.42	− 73.81	− 75.48
ΔE_{tot}	− 48.41	− 57.28	− 65.77

2.2 Triply Hydrogen Bonded Systems

Model systems exhibiting the three different triple hydrogen bonding motifs are illustrated in Figure 3. Experimental data suggest that complexes of the AAA.DDD type have the highest association constants, while those of the ADA.DAD type are considerably lower.[18] On the basis of SPT-type calculations,[12b] the trend in association energies has been interpreted by Jorgensen and co-workers in terms of differences in the secondary electrostatic interactions, illustrated in Figure 3. In the AAA.DDD system, all four secondary interactions are attractive, in AAD.DDA, two are attractive and two are repulsive, while in ADA.DAD, all four are repulsive.

The results of DFT calculations on the three model systems are illustrated in Figure 4.[19] Once again the DFT methodology predicts the correct order of bonding energies, with the AAA.DDD complex the most stable. The energy decomposition (summarized in Table 2 for $r = 1.8$ Å and $r = 4.5$ Å) reveals that the underlying cause of the different stabilities is rather more subtle than in the comparison of imides and lactams described above. At an intermolecular separation of 4.5 Å, the total energy is almost entirely dominated by the long range electrostatic term. In the vicinity of the energy mimina ($r = 1.8$ Å), however, differences in ΔE_{oi} exert a significant influence on the relative

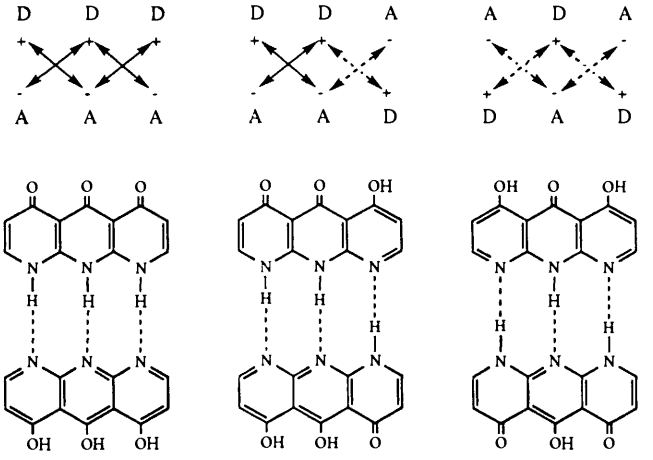

Figure 3 Model systems exhibiting three different triple hydrogen bonding motifs.

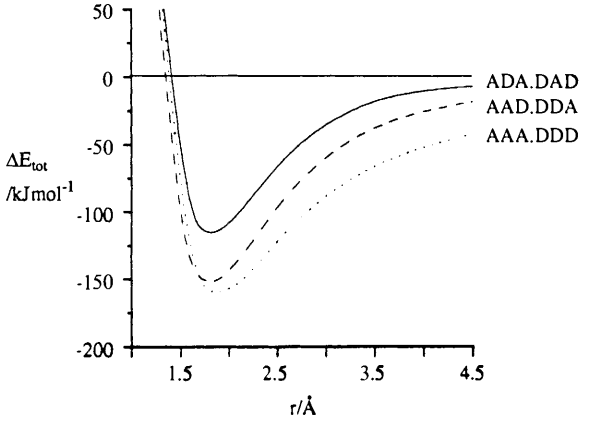

Figure 4 Total energy *versus* hydrogen bond distance for the three triple hydrogen bonding motifs.

values of the total energy. As explained previously, the orbital interaction term reflects the ability of the two interacting systems to respond to changes in their environment by redistribution of electronic density. Table 2 indicates that this reorganization is most favourable for the AAD.DDA complex. Furthermore, the changes in ΔE_{oi} occur almost entirely within orbitals which are antisymmetric with respect to the molecular plane – *i.e.* within the delocalized π system. Cooperative π effects, which have been proposed by several authors,[18b,20] are able to enhance the hydrogen bonding interaction in ADA.DAD and AAD.DDA, but not in AAA.DDD systems. The results summarized in Table 2 suggest that these cooperative effects are indeed significant, and account for the enhanced ΔE_{oi} term in the AAD.DDA complex relative to AAA.DDD.

The reasons for the low ΔE_{oi} term in the ADA.DAD system, where π cooperativity is also possible, are less clear. In AAD.DDA (C_s symmetry), a bulk redistribution of charge from one side of each molecular fragment to the other can occur,

Table 2

	$r = 1.8$ Å			$r = 4.5$ Å		
	ADA.DAD	AAD.DDA	AAA.DDD	ADA.DAD	AAD.DDA	AAA.DDD
ΔE_{el}	− 206.35	− 221.96	− 233.76	− 5.98	− 16.74	− 37.49
ΔE_{xrp}	241.42	237.19	231.67	0.59	0.75	0.71
ΔE_{oi}	− 150.16	− 166.86	− 156.48	− 1.09	− 1.84	− 4.81
ΔE_{tot}	− 115.09	− 151.63	− 158.57	− 6.48	− 17.83	− 41.59

compensating for the local loss or gain of electron density due to hydrogen bonding. The ADA.DAD motif has C_{2v} symmetry, and the presence of a symmetry axis perpendicular to the molecule plane prevents this bulk redistribution of charge, and may account for the rather small calculated orbital interaction term.

The contrast between the triply hydrogen bonded systems and the diimide/dilactam molecular pairs described previously is noteworthy. In the latter, the hydrogen bonding motif is identical in all cases, and so the redistribution of electron density is approximately constant across the series. In contrast, the three systems ADA.DAD, AAD.DDA, and AAA.DDD have different topologies, which permit different degrees of electronic relaxation, and consequently changes in the orbital interaction term become significant.

If, as in the case of the imide/lactam systems, differences in ΔE_{el} are equated with the secondary electrostatic interactions, we arrive at an estimate of approximately 7 kJ mol^{-1} per secondary interaction, somewhat smaller than the 10kJmol^{-1} for the imide/lactam systems. This may reflect the fact that, in the triply bonded systems, the groups responsible for the secondary interactions are also involved in primary hydrogen bonds with the other component of the molecular pair. In contrast, the carbonyl oxygens responsible for the destabilization of the diimides are entirely nonbonding, and are able to exert a greater destabilizing influence on the molecular pair.

2.3 Metal-mediated Effects on Hydrogen Bonding

The role of metal ions in supramolecular systems may simply be to act as a coordination centre, providing a template for the formation of a rigid framework of remote hydrogen bonding sites. Alternatively, the metal ion may exert an electronic effect on the individual proton donor and acceptor sites, influencing the hydrogen bonding in a more subtle manner. Complexes of biureto ($[C_2N_3O_2H_3]^{2-}$) and dithiobiureto ($[C_2N_3S_2H_4]^{1-}$) ligands (Figure 5) have surfaces suitable for triple hydrogen bonding interactions. The two ligands present rather different hydrogen bonding motifs to a probe molecule, biureto complexes having an ADA arrangement of sites, while in complexes of dithiobiuret, the arrangement is DAD. In Table 3, the total interaction energy is summarized for a range of biureto and dithiobiureto complexes with the complementary probe fragments shown in Figure 5.[19]

The most significant influence on the hydrogen bonding capability of each fragment is the overall charge. Molecular pairs involving the biureto complex (ADA) are most stable in the presence of neutral metal fragments such as $NiCl_2$, and least stable in the presence of cationic fragments such as $Ni(CO)_2^{2+}$.

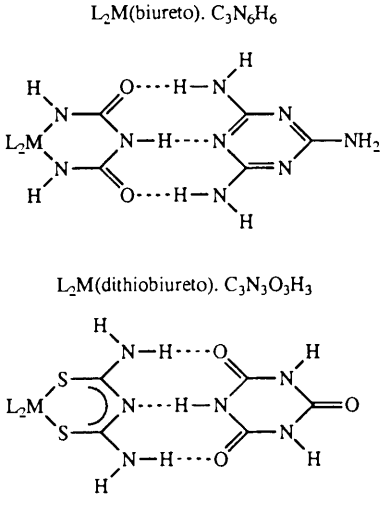

Figure 5 Biureto and dithiobiureto complexes used to model the hydrogen bonding to organic bases.

Table 3

	L_2M(biureto) Complexes			
L_2M	ΔE_{el}	ΔE_{xrp}	ΔE_{oi}	ΔE_{tot}
$NiCl_2$	− 171.80	210.58	− 136.73	− 97.86
$Ni(CN)_2$	− 171.46	209.99	− 133.80	− 95.27
$Ni(C_3N_3O_2H_3)$	− 171.84	210.08	− 134.14	− 95.90
H^+	− 165.39	205.27	− 117.57	− 77.70
$Ni(CO)_2^{2+}$	− 148.16	193.38	− 113.47	− 68.28
	L_2M(dithiobiureto) Complexes			
L_2M	ΔE_{el}	ΔE_{xrp}	ΔE_{oi}	ΔE_{tot}
$NiCl_2$	− 169.45	200.00	− 115.85	− 85.35
$Ni(CN)_2$	− 167.57	198.32	− 114.52	− 83.72
$Ni(C_3N_3S_2H_3)^+$	− 160.29	190.66	− 112.97	− 82.59
H^+	− 159.95	190.66	− 114.14	− 83.43
$Ni(CO)_2^{2+}$	− 146.82	178.49	− 123.43	− 91.84

The opposite trend is observed for dithiobiureto complexes (DAD), where the positive charge enhances the hydrogen bonding. Changes related to the π donor/acceptor properties of the ligand are less significant, as illustrated by the similarity of $NiCl_2$ and $Ni(CN)_2$ complexes.

The reduced hydrogen bonding capacity in positively charged complexes of the biuret ligand is consistent with the presence of an excess of proton acceptor groups. Electron density is withdrawn from the electron-rich carbonyl groups, thereby reducing both the electrostatic and orbital interaction terms, resulting in a substantially lower total interaction energy in the $Ni(CO)_2^{2+}$ complex.

The trends within the series of dithiobiureto complexes are rather more difficult to explain. In contrast to the biureto systems, the hydrogen bonding is enhanced in the presence of a positive charge, but the effect is far more marginal. In addition, the electrostatic interaction is *reduced*, despite the presence now of an excess of proton donor groups. The reason for this counter-intuitive observation lies in the different influence of the coordinated metal centre on proton donor and acceptor groups. The nitrogen atom at the central proton acceptor site is linked directly to the metal centre *via* a conjugated π system, while the protons on the amine groups are separated from the π system by an N−H σ bond. The buffering effect of this σ bond renders the proton donor groups considerably less sensitive to the electronic influence of the remote coordination site than their proton accepting counterparts. In the case of the dithiobiureto complexes, the reduction in the electrostatic interaction at the central proton acceptor site is considerably greater than the cumulative enhancement at the acceptor sites, despite the presence of two of the latter.

In terms of supramolecular chemistry, and particularly the possibility of selectively 'tuning' hydrogen bonds, these results suggest that attempts to influence the interaction of two molecular fragments through modification of the proton acceptor groups will meet with more success than the alternative strategy of influencing the proton donors.

3 Experimental Results

3.1 Complexes with DAD Hydrogen Bonds

3.1.1 Dithiobiureto Complexes

The ligand dithiobiuret (Hdtb) forms neutral S,S′ complexes with nickel, palladium, and platinum,[21] which possess an arrangement of hydrogen bonds DAD capable of base pairing with ADA complementary organic bases. Through the judicious choice of complementary bases, in terms of steric bulk, additional hydrogen bonding sites, aromaticity, *etc.*, the dimensionalities of the intermolecular interactions can be varied. Scheme 1 illustrates how the complementary interactions may be utilised for the construction of isolated assemblies, molecular tapes of

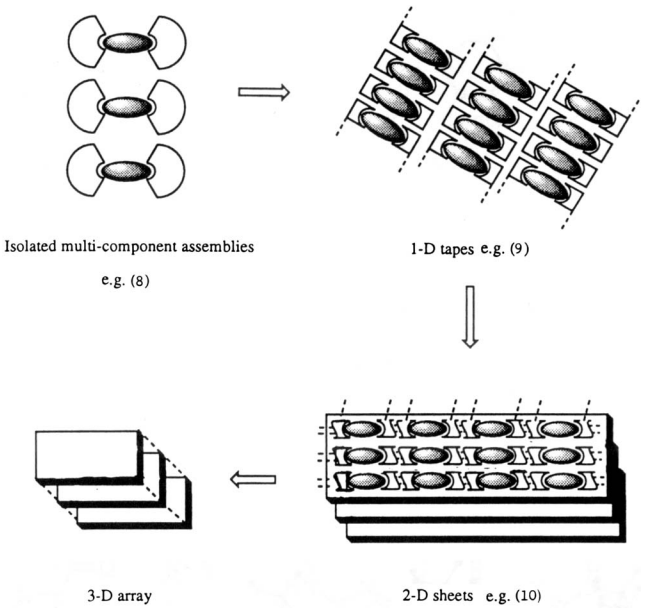

Scheme 1

sheets, and a 3D matrix structure. Specifically co-crystals of the metal complex $[Ni(dtb)_2]$ with the complementary organic molecules 1,8-naphthalimide (8),[22] bemigride (9),[22] and uracil (10),[23] have been studied. The co-crystals (8)—(10) display self assembly of their components *via* triple complementary hydrogen bonding interactions. However, the three-dimensional crystal structures are quite different with (8) containing essentially an isolated three-component assembly, (9) displaying nano-scale molecular tapes which include the Ni complex in a unique planar arrangement, and (10) forming sheets with cross-linking between adjacent tapes.

In $[Ni(dtb)_2$:(1,8-naphthalimide)$_2]$ (8) the 1,8-naphthalimide acts as a terminating group (Figure 6), supressing the formation of extended inter-complex NH···N bonded chains which predominate in the crystal structures of other $[M(dtb)_2]$ complexes (where M = Ni, Pd, Pt). The hydrogen bonding distances are 2.867 and 2.915 Å for NH···O and 3.113 Å for NH···N interactions. The *exo*-NH protons are not involved in any significant hydrogen bonding, the closest approaches to any C=O groups being 3.298 and 3.354 Å. There are no aromatic stacking interactions and thus co-crystal (8) may be identified as an example of an isolated multimolecular assembly.

The smaller size of the bemigride molecule in $[Ni(dtb)_2$:(bemigride)$_2]$ (9) modifies the crystal packing and permits additional intermolecular interactions. These involve hydrogen bonding of the *exo*-NH proton to the carbonyl oxygen atoms of adjacent, in plane, $[Ni(dtb)_2$:(bemigride)$_2]$ units and thereby forming molecular tapes (Figure 7). These tapes have a width of 2nm (19.2Å) and propagate along the crystallographic *a*-axis. The tapes are packed in an interacting herring-bone fashion (Figure 8) with minimum edge-to-face and face-to-face separations of 3.5 Å. Thus in (9), six of the eight protons of $[Ni(dtb)_2]$ are involved in strong hydrogen bonds to bemigride molecules. Within the tapes the two remaining NH protons are directed towards the sulfur atoms of adjacent $[Ni(dtb)_2$:(bemigride)$_2]$ units.

On replacing bemigride by uracil (10), further hydrogen bonding interactions become possible because of the additional

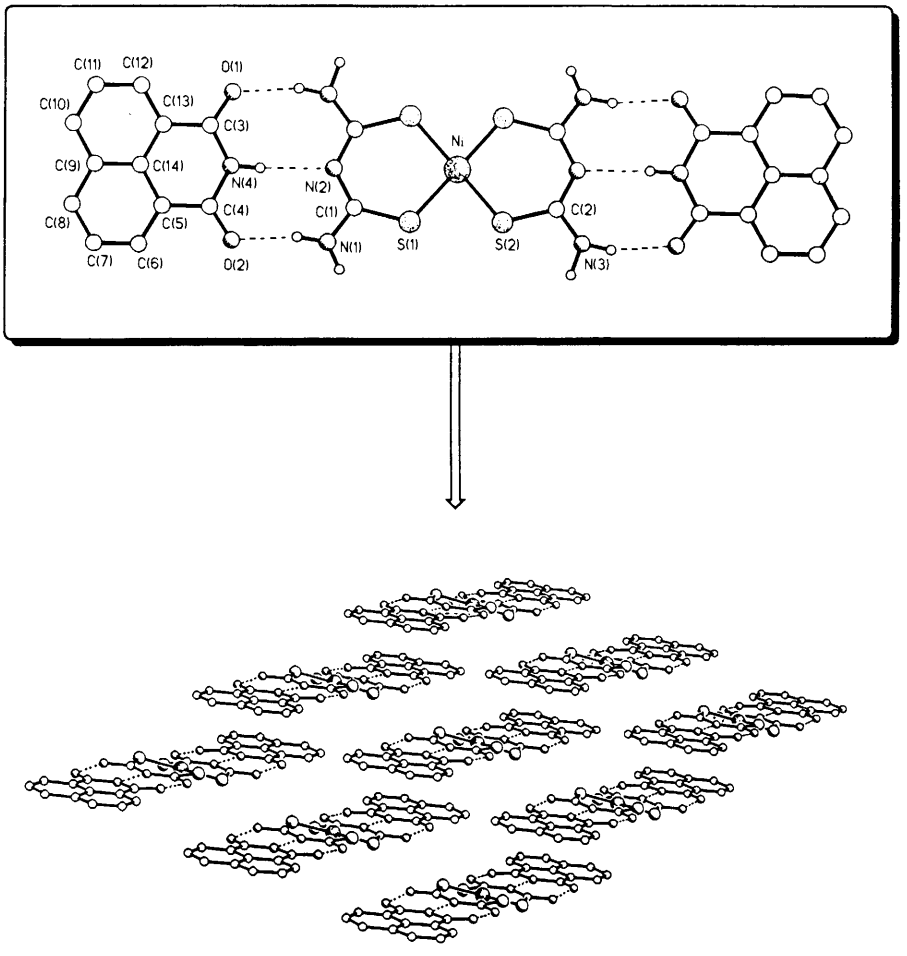

Figure 6 The self-assembled unit of (8) illustrating the complementary triple hydrogen bonding interactions, and molecular packing of the isolated 1 + 2 assemblies.

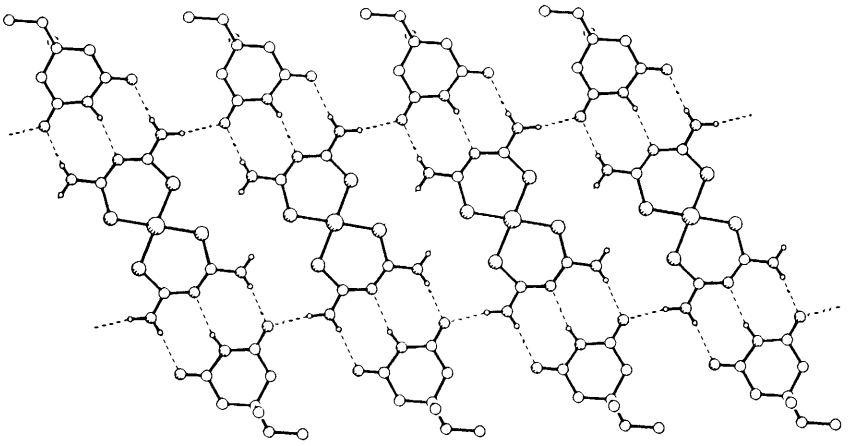

Figure 7 A section of the molecular 'metallo-tape' in (9).

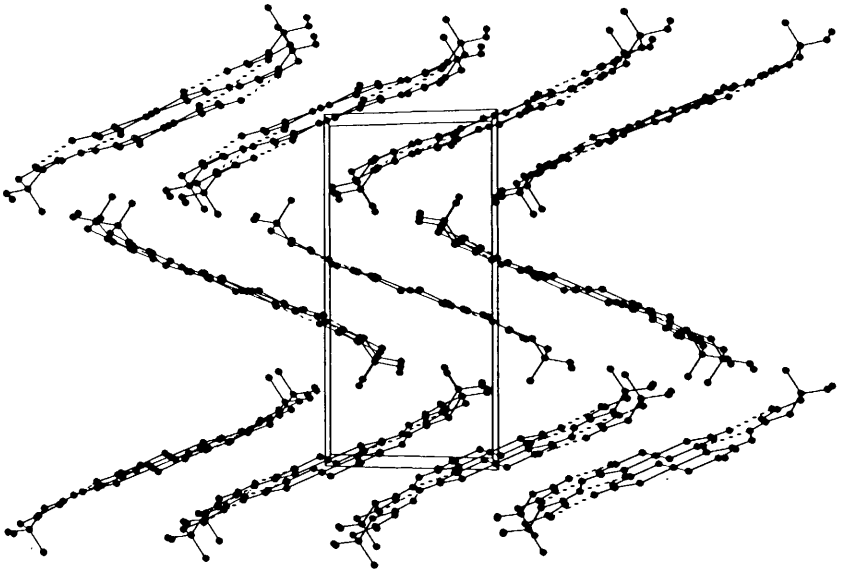

Figure 8 Herring-bone packing of the 'tapes' in (9).

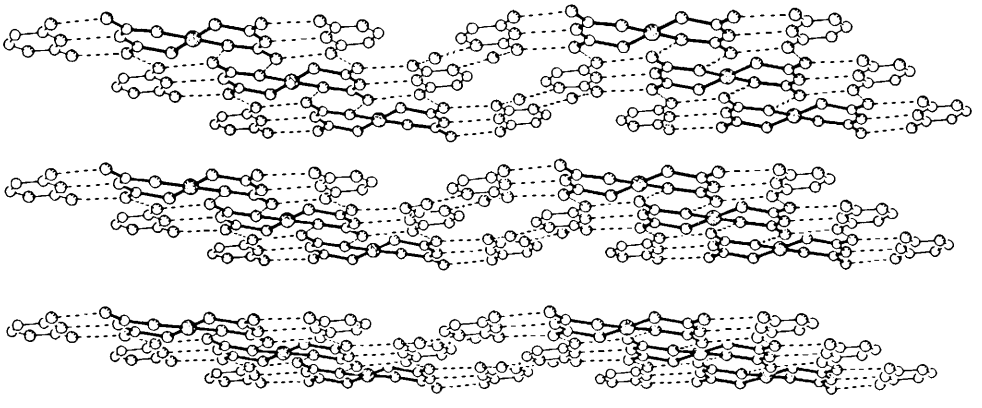

Figure 9 Sheet structure of (10). Spacer included water molecules link the tapes in addition to the intermolecular hydrogen bonds.

ring NH group (Figure 9). The conditions for tape formation are unchanged but the presence of the additional NH group permits cross-linking between adjacent tapes creating a sheet structure. The cross-linking between tapes requires the presence of additional hydrogen bonding H_2O spacer molecules. In common with (9), only six of the eight dtb hydrogen atoms are involved in hydrogen bonding with the other two directed towards the sulfur atoms of the adjacent molecules.

3.1.2 Pyridyl-2,4-diamino-1,3,5-triazine Complexes

Only a few 1,3,5-triazine metal complexes has been reported in the literature,[24] probably because the ligand is readily hydrolysed. Lerner and Lippard[25] revealed that 2,4,6-tris(2-pyrimidyl)- and 2,4,6-tris(2-pyridyl)-1,3,5-triaines were hydrolysed in the presence of divalent copper to give *bis*(arylcarbonyl)aminatocopper(II) complexes and the free arylamides.

The series of pyridyl-2,4-diamino-1,3,5-triazines shown in Figure 10 have been prepared and fully characterized and they possess both metal coordinating and hydrogen bonding capabilities.[26] All these ligands were prepared by heating the arylamide with the corresponding biguanide in methanol (Scheme 2). Thus, condensation of 4-pyridinecarboxamide with biguanide afforded 4-pyridyl-2,4-diamino-1,3,5-triazine in 50% yield. The yields of some of the ligands can be as high as 90%.

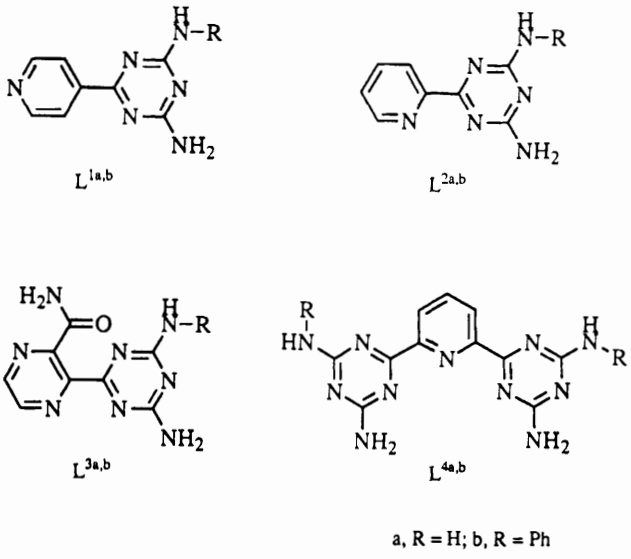

Figure 10 The series of pyridyl-2,4-diamino-1,3,5-triazines that have been synthesized.

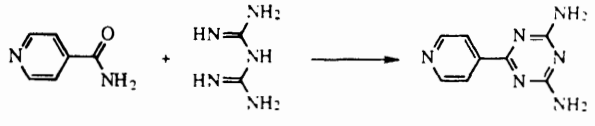

Scheme 2

The crystal structure of 6-(4-pyridyl)-2-phenylamino-4-amino-1,3,5-triazine[26] (Figure 11) shows that the molecules adopt a head-to-tail arrangement with the phenylamino-hydrogen bonded to the pyridine nitrogen. The phenyl ring points away from the other amino-group. Water molecules are incorporated in the lattice, and act as hydrogen bond donors to the triazine nitrogens and as hydrogen bond acceptors to the remaining amino-hydrogens.

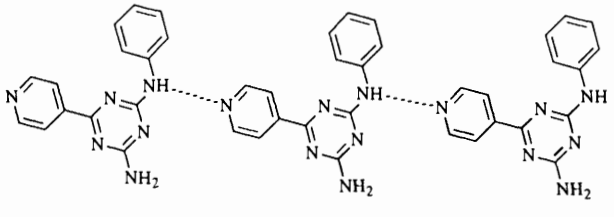

Figure 11 Hydrogen bonding observed within 6-(4-pyridyl)-2-phenylamino-4-amino-1,3,5-triazine (L^{1b}).

Blue crystals have been obtained from a dimethylsulfoxide solution of copper(II) perchlorate and 6-(4-pyridyl)-2,4-diamino-1,3,5-triazine (2 eq.). A crystal structure analysis[26] indicates that the metal centre is coordinated to four solvent molecules and two pyridyl rings which are *cis* to each other. Although the solvent molecules and counter anions are extremely disordered, a zig-zag chain of hydrogen bonded pyridyl-diaminotriazine copper complexes is well defined (Figure 12).

Chelating triazine complexes have been synthesized by replacing the *para* substituted pyridine with an *ortho* pyridine (Scheme 3).

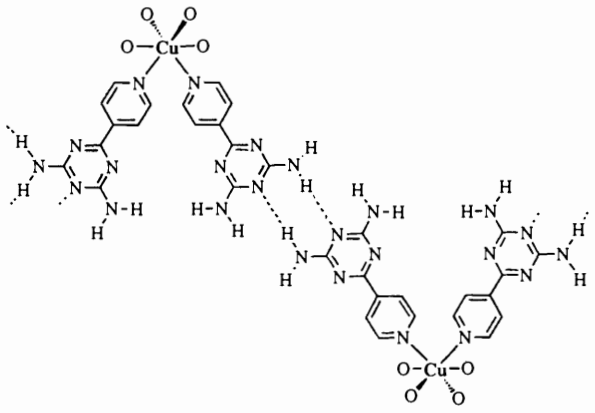

Figure 12 Hydrogen bonding observed within *cis*-$[Cu(dmso)_4(L^{1a})_2](ClO_4)_2$ resulting in zig-zag chains.

6-(2-pyridyl)-2,4-diamino-1,3,5-triazine (L^{2a}) reacts with sodium tetrachloropalladate in water giving $[PdL^{2a}_2]Cl_2$, which is water soluble, and no degradation of this complex was observed after heating in boiling water for several days. Reaction with dichlorobis(benzonitrile)palladium in hot acetonitrile leads to $[PdL^{2a}Cl_2]$. Both compounds of L^{2a} have melting points higher than 300 °C. Possibilities for configurational isomerism arise in the case of $[PdL^{2a}_2]Cl_2$ and when one of the amino groups is substituted as in L^{2b}. The structural similarity of L^{2a} and 2,2′-bipyridine suggests many interesting possibilities for future development, not only of crystal engineering but also in the intercalation reactions involving DNA.

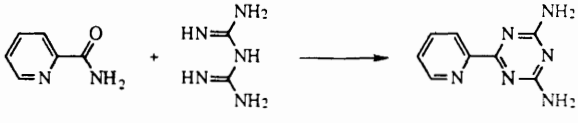

Scheme 3

3.2 Complexes with ADA Hydrogen Bonds

3.2.1 Orotic Acid Complexes

Another ligand containing a combination of hydrogen bond donors and acceptors is the dianion based on orotic acid (2,6-dioxo-1,2,3,6-tetrahydro-4-pyrimidine carboxylic acid):

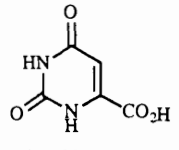

orotic acid (H_2orot)

This has the ability to act as a bidentate ligand whilst retaining the hydrogen bond acceptor, donor, acceptor (ADA) arrangement. Tetra-aqua orotate complexes of nickel, copper, and zinc have been previously reported.[27] We have shown that these compounds co-crystallize with a variety of molecules with complementary hydrogen bonding groups, including adenine and melamine. Single crystals have been obtained from [Ni(orot)$(OH_2)_4$] and melamine. The crystal structure[28] shown in Figure 13 illustrates that, as expected, the two molecules are linked by three hydrogen bonds between the C(**O**)–N**H**–C(**O**) moiety of the orotate and the NH_2–C–**N**–C–NH_2 moiety of one face of the melamine. These 1 + 1 units are linked into tapes by hydrogen bonds between the third amino group on the melamine and both a carboxylate oxygen and one aquo oxygen

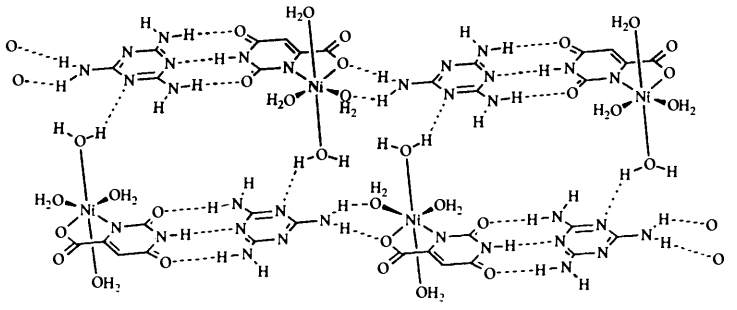

Figure 13 Hydrogen bonding observed within $[Ni(orot)(OH_2)_4]\cdot$melamine showing molecular tapes linked together by hydrogen bonds to the axial water molecules.

on another $[Ni(orot)(OH_2)_4]$ molecule. Further hydrogen bonding between the axial water molecules and both triazine nitrogen atoms and other water molecules link together these tapes.

New bis(phosphine) orotate complexes of palladium and platinum have been made from $[M(cod)Cl_2]$ (M = Pd and Pt) as below,[28] using the method of Kemmitt *et al.*[29] to abstract the chloride ligands (Scheme 4).

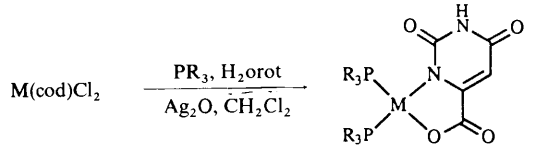

M = Pt; PR_3 = PPh_3, PMe_2Ph, PEt_3, 0.5 dppe
M = Pd; PR_3 = 0.5 dppe

Scheme 4

The chemical shift of N(3)–**H** in the ^{1}H-NMR spectrum is concentration dependent in $CDCl_3$, suggesting an equilibrium between the monomer and a di-hydrogen bonded dimer. Such a dimer is observed in the crystal structure of $[Pt(PPh_3)_2(orot)]$, shown in Figure 14.

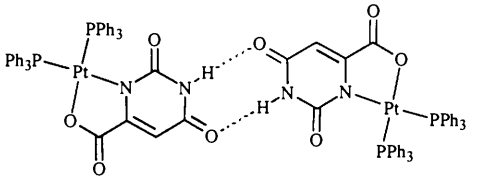

Figure 14 Hydrogen bonded dimers observed in the crystal structure of $[Pt(PPh_3)_2(orot)]$.

The *X*-ray crystal structure of a co-crystal obtained from [Pt(dppe)(orot)] and 2,6-diaminopyridine shows the presence of a 2 + 2 aggregate. Each [Pt(dppe)(orot)] molecule is bound through three hydrogen bonds to a 2,6-diaminopyridine molecule, then these 1 + 1 units are linked in a head-to-tail manner with additional hydrogen-bonding between an amino proton and a carbonyl group to give the 2 + 2 adduct (Figure 15). Further hydrogen bonding to produce an extended structure is prevented by the diphosphine ligands which act as blocking groups. The 1 + 1 adduct is additionally stable enough to be observed in the FAB mass spectrum.

It is interesting to compare the chemistry of the platinum orotate compounds with their analogues based on 5-aminoorotic acid:

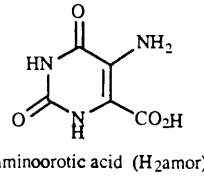

5-aminoorotic acid (H_2amor)

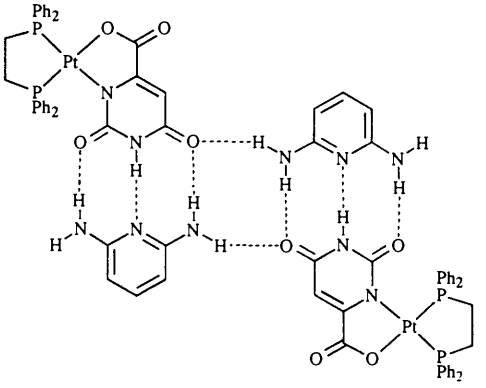

Figure 15 The 2 + 2 assembly observed in the crystal structure of [Pt(dppe)(orot)]·(2,6-diaminopyridine).

The same reaction as before now gives two isomeric products, one containing a 5-membered chelate ring as before and the other containing a 6-membered chelate ring (Scheme 5).[28]

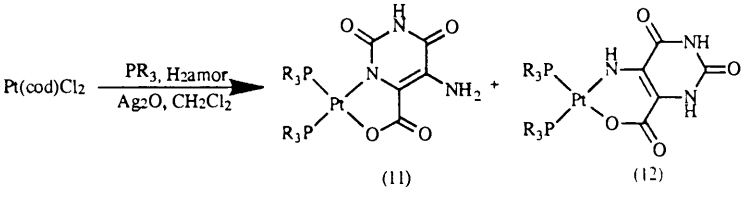

Scheme 5

The novel isomers have been isolated by fractional crystallization and identified from the ^{1}H-NMR [$^2J_{Pt,H}$ satellites are observed for (12)]. Both compounds retain ADA hydrogen-bonding groups on their surface, but their geometric arrangements relative to the square-plane are quite different. The two isomers slowly equilibrate in $CDCl_3$ with an equilibrium constant of 2.1 in favour of the 5-membered ring containing isomer (11) for the PPh_3 complexes. Both complexes have been characterized by *X*-ray crystallography and show important differences in their solid-state structures. Structure (11) exists as a hydrogen-bonded tetramer (Figure 16) whereas (12) occurs as a hydrogen-bonded dimer (Figure 17) but with different carbonyls involved on each molecule.

The self-assembled tetrameric structure observed for (11) is reminiscent of the structure of guanine tetraplexes[30] which have similar hydrogen-bonding patterns and are stabilized by a central sodium ion. Reaction of either isomer of $[Pt(PPh_3)_2$(amor)] with Na^+ does not lead to an alkali metal ion stabilized tetramer, as may have been expected, but to the diplatinum molecule shown in Figure 18.[28] In this compound both faces of the 5-aminoorotate ligand are being utilised so that both 5- and 6-membered rings are formed. Overall the ligand is acting as a trianion so the complex is overall cationic. This complex forms

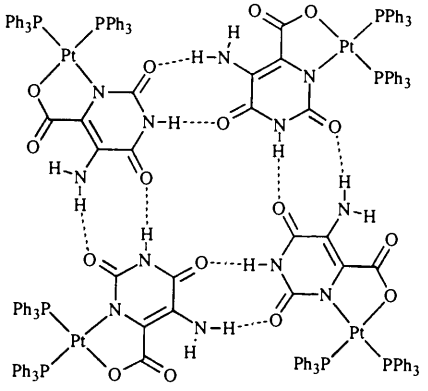

Figure 16 Hydrogen bonded tetramers observed in the crystal structure of (11).

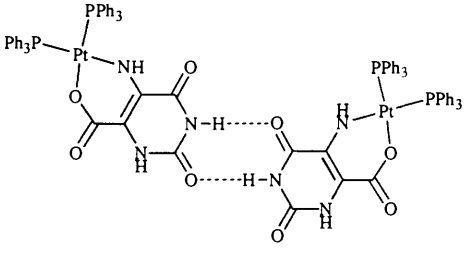

Figure 17 Hydrogen bonded dimers observed in the crystal structure of (12).

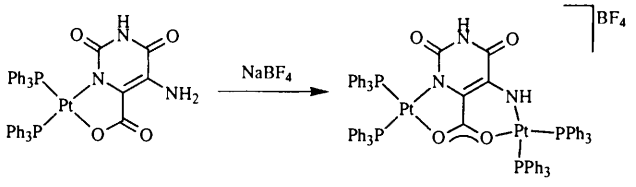

Figure 18 Reaction of either isomer of $[Pt(PPh_3)_2(amor)]$ with $NaBF_4$ gives the diplatinum complex shown.

hydrogen-bonded dimers in the solid state with two hydrogen bonds linking the molecules.

3.2.2 Complexes of 5-(2-pyridylmethylene)hydantoin

5-(2-pyridylmethylene)hydantoin (pyhyH) has the desired conformation and bite angle to form stable complexes with transition metals:

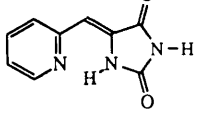

5-(2-pyridylmethylene)hydantoin

(pyhyH)

These complexes retain the ability to form complementary hydrogen bonds with nucleotide bases through the C(**O**)–NH–C(**O**) moiety. Indeed, hydantoins substituted at the C-5 position have a remarkably wide range of pharmacological activities including anticonvulsant,[31] antidepressant,[32] and platelet aggregation inhibitory activities.[33]

The stereoisomerically pure *Z*-form of pyhyH[34,35] was synthesized using a new high yield method[36] which involves the condensation of hydantoin with 2-pyridylcarboxyaldehyde. We have found that piperidine used both as a base and solvent at high temperatures gave exclusively *Z*-pyhyH in greater than 70% yield (Scheme 6).

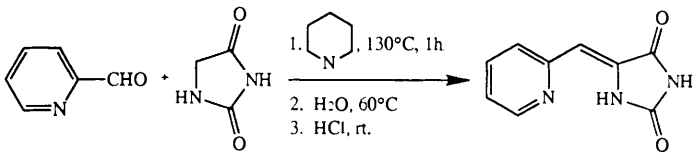

Scheme 6

Crystallographic studies have confirmed the planarity of the structure and the formation of a delocalized system incorporating the N(1)H atom as proposed by Tan.[37] The packing arrangement of pyhyH results from the stacking of planar sheets formed by hydrogen bonding interactions between the molecules (Figure 19).

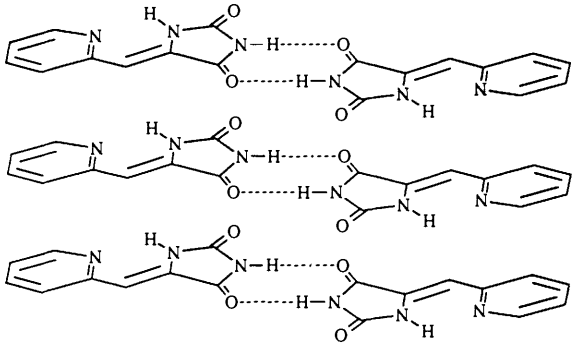

Figure 19 Packing arrangement in the crystal structure of pyhyH.

Surprisingly, no metal complexes of pyhy have been reported despite its obvious similarity with bipyridyl and phenanthroline. The reactions summarized in Figure 20 have yielded a wide range of complexes of this ligand.

$CuCl_2 \cdot 2H_2O$ + pyhyH	MeOH/H_2O, 1h reflux	$[Cu(pyhy)_2]$
$CuCl_2 \cdot 2H_2O$ + pyhyH	MeOH/H_2O, 5 mins stir	$[Cu(pyhy)(Cl)(OH_2)]$
$Ni(ClO_4)_2$ + pyhyH	MeOH/H_2O, 1h reflux	$[Ni(pyhy)(OH_2)_4]$
$Pd(OAc)_2$ + pyhyH	MeOH/H_2O, 2h reflux	$[Pd(pyhy)_2]$
$[RhCl(CO)_2]_2$ + pyhyH	MeCN/N_2, 10 mins stir	$[Rh(pyhy)(CO)_2]$
$RuCl_3 \cdot H_2O$ + pyhyH	MeOH, reflux	$[Ru(pyhy)_3]$
$Ni(OAc)_2 \cdot 4H_2O$ + pyhyH	Naphthalene, 80°C/2h	$[Ni(pyhy)_2]$
$Pd(PhCN)_2Cl_2$ + pyhyH	MeOH, 10h reflux	$[Pd(pyhy)_2]$

Figure 20 Reactions of pyhyH, summarizing the wide range of complexes which may be formed from it.

The ability of the complexes to form supramolecular aggregates with nucleotide and related bases which are able to form complementary hydrogen bonds with the C(**O**)–NH–C(**O**) moiety is hampered by their poor solubilities. Microwave dielectric heating which superheats the solutions by 70—100°C improves their solubility characteristics significantly. When the

$CuCl_2 \cdot 2H_2O$ + pyhyH + melamine

MeOH, 130°C, microwaves, 1h

$Cu(pyhy)_2 \cdot 2$melamine
80%,
green-red dichroic
crystals

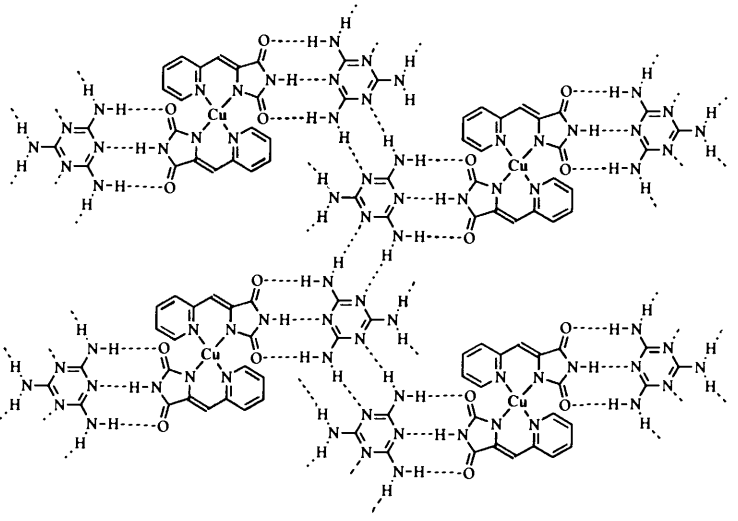

Figure 21 Hydrogen bonding array observed in the crystal structure of $[Cu(pyhy)_2]\cdot 2$melamine.

reaction was carried out in the presence of a complementary hydrogen-bonding component, crystals satisfactory for single crystal *X*-ray analysis were obtained.

The novel structure of this molecular aggregate[36] is shown in Figure 21. This shows a four coordinate copper(II) centre with two chelated ligands adopting a distorted tetrahedral geometry. Each ligand in this neutral complex triply hydrogen bonds to a melamine molecule. These melamine units hydrogen bond to neighbouring melamines and thereby form an array. These arrays are arranged in a 'double layered crinkle sheet' arrangement where two complex units and two melamine units assemble *via* eight hydrogen bonds and eight coordinate bonds to form a ring.

4 Conclusions

This research has confirmed that it is possible to form a wide range of bifunctional transition metal complexes based on ligands which can simultaneously form stable and inert metal–ligand bonds and have recognition sites on their surface which complement those found in nucleic acid bases. In particular, complexes with DAD and ADA hydrogen-bonding recognition sites have been synthesized and shown to form co-crystals with a wide range of organic bases. The strength of the hydrogen bonding is influenced in a subtle manner by the metal atom and the effects have been quantified using density functional theory calculations. The synthesis and characterization of these bifunctional transition metal complexes has significant implications both for crystal engineering studies and also the design of new chemotherapeutic molecules.

Acknowledgements. We thank BBSRC for financial support and BP plc for endowing DMPM's chair. The crystallographic contributions of Drs. D. J. Williams and A. J. P. White are gratefully acknowledged.

5 References

1 J.-M. Lehn, *Angew. Chem., Int. Ed. Engl.*, 1988, **27**, 89.
2 (*a*) D. M. Huryn and M. Okabe, *Chem. Rev.*, 1992, **92**, 1745; (*b*) C. H. Schwalbe, D. R. Lowis, and W. G. Richards, *J. Chem. Soc., Chem. Commun.*, 1993, 1199.
3 (*a*) G. M. Whitesides, E. E. Simanek, J. P. Mathias, C. T. Seto, D. N. Chin, M. Mammen, and D. M. Gordan, *Acc. Chem. Res.*, 1995, **28**, 37; (*b*) D. Braga, F. Grepioni, K. Biradha, V. R. Pedireddi, and G. R. Desiraju, *J. Am. Chem. Soc.*, 1995, **117**, 3156.
4 (*a*) J. A. Zerkowski, C. T. Seto, and G. M. Whitesides, *J. Am. Chem. Soc.*, 1990, **112**, 9025; (*b*) C. T. Seto and G. M. Whitesides, *J. Am. Chem. Soc.*, 1991, **113**, 712; (*c*) J. A. Zerkowski, C. T. Seto, and G. M. Whitesides, *J. Am. Chem. Soc.*, 1992, **114**, 5473; (*d*) C. T. Seto and G. M. Whitesides, *J. Am. Chem. Soc.*, 1993, **115**, 905; (*e*) C. T. Seto, J. P. Mathias, and G. M. Whitesides, *J. Am. Chem. Soc.*, 1993, **115**, 1321.
5 (*a*) J.-M. Lehn, M. Mascal, A. DeCian, and J. Fischer, *J. Chem. Soc., Chem. Commun.*, 1990, 479; (*b*) J.-M. Lehn, M. Mascal, A. DeCian, and J. Fischer, *J. Chem. Soc., Perkin Trans. 2*, 1992, 461.
6 (*a*) S. K. Chang and A. D. Hamilton, *J. Am. Chem. Soc.*, 1988, **110**, 1318; (*b*) S. J. Geib, S. C. Hirst, C. Vincent, and A. D. Hamilton, *J. Chem. Soc., Chem. Commun.*, 1991, 1283; (*c*) F. Garcia-Tellado, S. J. Geib, S. Goswami, and A. D. Hamilton, *J. Am. Chem. Soc.*, 1991, **113**, 9265; (*d*) E. Fan, S. A. Van Arman, S. Kincaid, and A. D. Hamilton, *J. Am. Chem. Soc.*, 1993, **115**, 369; (*e*) S. J. Geib, C. Vicent, E. Fan, and A. D. Hamilton, *Angew. Chem., Int. Ed. Engl.*, 1993, **32**, 119.
7 M. C. Etter, *Acc. Chem. Res.*, 1990, **23**, 120.
8 C. B. Aakeröy and K. R. Seddon, *Chem. Soc. Rev.*, 1993, **22**, 397.
9 J. C. MacDonald and G. M. Whitesides, *Chem. Rev.*, 1994, **94**, 2383.
10 S. Subramanian and M. J. Zaworotko, *Coord. Chem. Rev.*, 1994, **137**, 357.
11 P. Hobza, J. Sponer, and M. Polasek, *J. Am. Chem. Soc.*, 1995, **117**, 792.
12 (*a*) W. L. Jorgensen and D. L. Severance, *J. Am. Chem. Soc.*, 1991, **113**, 209; (*b*) J. Pranata, S. G. Wierschke, and W. L. Jorgensen, *J. Am. Chem. Soc.*, 1991, **113**, 2810.
13 T. Ziegler, *Chem. Rev.*, 1991, **91**, 651.
14 (*a*) F. Sim, A. St.-Amant, I. Papai, and D. R. Salahub, *J. Am. Chem. Soc.*, 1992, **114**, 4391; (*b*) M. Kieninger and S. Suhai, *Int. J. Quantum Chem.*, 1994, **52**, 465.
15 T. Ziegler and A. Rauk, *Theor. Chim. Acta*, 1977, **46**, 1.
16 (*a*) S. E. Krikorian, *J. Phys. Chem.*, 1982, **86**, 1875; (*b*) J. Hine, S. Hahn, and J. Hwang, *J. Org. Chem.*, 1988, **53**, 884; (*c*) K. S. Jeong, T. Tjivikua, A. Muehldorf, G. Deslongchamps, M. Famulok, and J. Rebek Jr., *J. Am. Chem. Soc.*, 1991, **113**, 201.
17 J. E. McGrady and D. M. P. Mingos, *J. Chem. Soc., Perkin Trans. 2*, submitted for publication.
18 (*a*) T. J. Murray and S. C. Zimmerman, *J. Am. Chem. Soc.*, 1992, **114**, 4010; (*b*) S. C. Zimmerman and T. J. Murray in 'Computational Approaches to Supramolecular Chemistry', Kluwer Academic Publishers, The Netherlands, 1994, p. 109.
19 J. E. McGrady and D. M. P. Mingos, unpublished results.
20 G. A. Jeffrey and W. Saenger, 'Hydrogen Bonding in Biological Structures', Springer-Verlag, Germany, 1994.
21 K. K. Chatterjee, *Z. Phys. Chem. (Frankfurt am Main)*, 1974, **89**, 88.
22 A. Houlton, D. M. P. Mingos, and D. J. Williams, *Transition Met. Chem.*, 1994, **19**, 653.
23 A. Houlton, D. M. P. Mingos, and D. J. Williams, *J. Chem. Soc., Chem. Commun.*, 1994, 503.
24 W. Kaufmann, L. M. Venanzi, and A. Albinati, *Inorg. Chem.*, 1988, **27**, 1178 and references therein.
25 E. I. Lerner and S. J. Lippard, *Inorg. Chem.*, 1977, **16**, 1546.
26 C.-W. Chan, D. M. P. Mingos, A. J. P. White, and D. J. Williams, unpublished results.
27 A. Karipides and B. Thomas, *Acta Cryst., C (Cr. Str. Commun.)*, 1986, **42**, 1705.

28 A. D. Burrows, D. M. P. Mingos, A. J. P. White, and D. J. Williams, manuscript in preparation.
29 R. D. W. Kemmitt, S. Mason, J. Fawcett, and D. R. Russell, *J. Chem. Soc., Dalton Trans.*, 1992, 1165.
30 G. Laughlan, A. I. H. Murchie, D. G. Norman, M. H. Moore, P. C. E. Moody, D. M. J. Lilley, and B. Luisi, *Science*, 1994, **265**, 520.
31 N. B. Mehta, C. A. Risinger Diuguid, and F. E. Soroko, *J. Med. Chem.*, 1981, **24**, 465.
32 F. L. Wessels, T. J. Schwan, and S. F. Pong, *J. Pharm. Sci.*, 1980, **69**, 1102.
33 A. G. Caldwell, C. J. Harris, R. Stepney, and N. Whittaker, *J. Chem. Soc., Perkin Trans. 1*, 1980, 495.
34 S.-F. Tan, K.-P. Ang, and G.-F. How, *J. Phys. Org. Chem.*, 1990, **3**, 559.
35 N. A. Meanwell, H. R. Roth, E. C. R. Smith, D. L. Wedding, and J. J. K. Wright, *J. Org. Chem.*, 1991, **56**, 6897.
36 M. M. Chowdhry, A. D. Burrows, D. M. P. Mingos, A. J. P. White, and D. J. Williams, *J. Chem. Soc., Chem. Commun.*, 1995, 1521; and unpublished results.
37 S.-F. Tan, K.-P. Ang, and G.-F. How, *J. Phys. Org. Chem.*, 1990, **3**, 703.